
ENERGY SPECTRUM OF AN ELECTRON WITH PHONON REPLICAS IN A FLAT SEMICONDUCTOR NANOHETEROSTRUCTURE WITH QUANTUM WELL

V.M. KRAMAR, M.V. TKACH

PACS 63.20.Kr; 79.60.Jv
©2010

Yu. Fedkovych Chernivtsi National University
(2, Kotsyubyns'kyi Str., Chernivtsi 58012)

We investigated the renormalization of the energy spectrum of an electron in a flat semiconductor nanoheterostructure with a rectangular quantum well of finite depth due to its interaction with optical polarization phonons. The analytical form of the mass operator with regard for two-phonon processes of the electron-phonon interaction at $T = 0$ K is obtained in the framework of the Green function method. The corrections to the main-band bottom energy of an electron and positions of the first phonon replicas induced by its interaction with confined, half-space, and interface phonons are calculated.

1. Introduction

The perspective to create modern electron-optical devices based on semiconductor nanoheterosystems (quantum wells (QW), dots, and wires) stimulates active searches for technologies of producing such systems and studies of their properties [1–5]. To a large degree, physical properties of nanosystems are determined by the structure of the energy spectrum of electrons and phonons, as well as by the efficiency of their interaction. They essentially depend on the spatial dimension of a nanosystem and external conditions. Thus, the study of regularities of the renormalization of the energy spectrum of electrons in nanosystems due to their interaction with phonons remains an urgent problem of both fundamental and applied investigations in the physics of low-dimensional systems.

Theoretical investigations of electron spectra in flat semiconductor nanoheterostructures with QWs (nanofilms, NF) with regard for their interaction with phonons are usually performed in the one-phonon ap-

proximation [6–11]. However, as is known from the theory of electron-phonon interaction (EPI) in bulky crystals, such an interaction can result in the appearance of bound states that manifest themselves as satellites of the fundamental band of the Raman spectrum (phonon replicas). Thus, there arises a need for the EPI theory in low-dimensional systems that would be able to consistently describe a wide energy range including the region of phonon replicas. Naturally, this theory must take into account multiphonon processes.

In the case of low concentrations of quasiparticles in a nanosystem, the problem of renormalization of the spectrum in a wide energy range is solved by the Green function method with the use of the Feynman–Pines diagram technique [13,14]. However, the problem consists in the fact that, in order to take multiphonon EPI processes into account, one must find the total mass operator (MO) of electrons that has a form of an infinite series of diagrams with all possible types and numbers of phonon lines. In the model of dispersion-free phonons, the sum of such a series can be obtained by means of the partial summation of the infinite series of diagrams with a fixed maximal number of virtual phonons in all orders relative to the coupling constant [15]. This procedure results in the integral-functional representation of the electron MO, whose practical use in specific problems represents an extremely complicated task.

This work aims at the adaptation of the integral-functional representation of the MO obtained in the general form in [15] to the calculation of the electron spectrum in NFs renormalized by EPI with regard for two-phonon processes. The solution of this problem allowed one to calculate, for the first time, the energy of the elec-

tron main-band bottom renormalized by EPI with all types of polarization optical phonons and gave a possibility to establish the position of bound electron-phonon states in NFs.

2. Hamiltonian of the Electron-Phonon System in a Flat Nanofilm. Renormalization of the Electron Spectrum at $T = 0$ K

Let us consider a flat nanofilm – a semiconductor with width a (medium “0”) placed into an external semiconductor medium (“1”) with a wider band-gap energy. The states of the electron system will be described in the effective-mass approximation, while those of the phonon one within the model of dielectric continuum. The further calculations are performed under the assumption about the nondegeneracy and the isotropy of the electron energy spectrum using the model of finite-depth rectangular QW.

Thus, in the coordinate system with the origin in the middle of the film and the XOY plane parallel to its surface, the effective mass m and the restricting potential V of an electron and the permittivity ε of the medium, where it is located, are supposed to be some known functions of the z -th component of the quasiparticle’s radius-vector:

$$m(z) = \begin{cases} m_0, & \varepsilon(z) = \begin{cases} \varepsilon^{(0)}, & V(z) = \begin{cases} 0, & |z| \leq \frac{a}{2}; \\ V, & |z| > \frac{a}{2}. \end{cases} \end{cases} \\ m_1, & \varepsilon^{(1)}, \end{cases}$$

The Hamiltonians of free electrons and phonons for such a model are obtained in [6–8]; the EPI Hamiltonian in the representation of occupation numbers over all variables of the system is also known [11].

In order to avoid too cumbersome mathematical calculations, we restrict ourselves to the consideration of the nanofilm with such a width, at which there exists the only electron band in the QW with the energy

$$E(\mathbf{k}) = E + \frac{\hbar^2 k^2}{2m},$$

where $\mathbf{k} = (k_x, k_y)$ is the two-dimensional quasimomentum of an electron. In this case, the Hamiltonian of the electron-phonon system in the representation of occupation numbers over all variables has the form

$$\hat{H} = \hat{H}_e + \hat{H}_{ph} + \hat{H}_{e-ph}, \quad (1)$$

where

$$\hat{H}_e = \sum_{\mathbf{k}} E(\mathbf{k}) \hat{a}_{\mathbf{k}}^+ \hat{a}_{\mathbf{k}} \quad (2)$$

is the electron Hamiltonian;

$$\begin{aligned} \hat{H}_{ph} = & \hat{H}_{L_0} + \hat{H}_{L_1} + \hat{H}_I = \sum_{\lambda, \mathbf{q}} \Omega_0 (\hat{b}_{\lambda, \mathbf{q}}^+ \hat{b}_{\lambda, \mathbf{q}} + 1/2) + \\ & + \sum_{q_{\perp}, \mathbf{q}} \Omega_1 (\hat{b}_{q_{\perp}, \mathbf{q}}^+ \hat{b}_{q_{\perp}, \mathbf{q}} + 1/2) + \sum_{\sigma, p, \mathbf{q}} \Omega_{\sigma, p} (\hat{b}_{\sigma, p, \mathbf{q}}^+ \hat{b}_{\sigma, p, \mathbf{q}} + 1/2) \end{aligned} \quad (3)$$

is the Hamiltonian of the system of polarization phonons in a nanoheterosystem: confined in the QW (L_0), whose states differ in values of the transverse component of the quasimomentum $q_{\lambda} = \lambda\pi/a$, where $\lambda = 1, 2, \dots, N = \text{int}(a/a_0)$, a_0 is the lattice constant of medium “0”; half-confined (L_1) in the barrier medium, and interface ones ($I_{\sigma p}$) – symmetric ($\sigma = s$) and antisymmetric ($\sigma = a$), high- ($p = +$) and low-energy ($p = -$) [6–8];

$$\begin{aligned} \hat{H}_{e-ph} = & \hat{H}_{e-L_0} + \hat{H}_{e-L_1} + \hat{H}_{e-I\sigma p} = \\ = & \sum_{\mathbf{k}, \mathbf{q}, \mu} F_{\mu}(\mathbf{q}) \hat{a}_{\mathbf{k}+\mathbf{q}}^+ \hat{a}_{\mathbf{k}} \hat{B}_{\mu \mathbf{q}} \end{aligned} \quad (4)$$

is the Hamiltonian of the electron interaction with all branches of optical polarization phonons in the QW ($\mu = L_0, L_1, I_{\sigma\pm}$). Here, $\mathbf{q} = (q_x, q_y)$ stands for the longitudinal quasimomentum of a phonon in a nanofilm; the rest of the notations are typical and are given in [11] together with the explicit form of the coupling functions $F_{\mu}(\mathbf{q})$.

According to the Green function theory [13,14], the electron spectrum at $T = 0$ K renormalized due to EPI is determined by the Fourier transform of the Green function

$$G(\omega, \mathbf{k}) = \frac{1}{\hbar\omega - E(\mathbf{k}) - M(\omega, \mathbf{k})}, \quad (5)$$

where $M(\omega, \mathbf{k})$ is the total MO [14, 15].

Taking into account the weakness of the electron-phonon coupling, we keep only the part of the total MO [15] describing two-phonon processes of electron scattering from the main band under the interaction with all phonon branches in a nanofilm [11]: confined, half-space, and symmetric interface (high- and low-energy) ones

$$\begin{aligned} M(\omega, \mathbf{k}) = \\ = \sum_{\mu, \mathbf{q}} \frac{|F_{\mu}(\mathbf{q})|^2}{\hbar\omega - E - \frac{\hbar^2}{2m_0} (\mathbf{k} + \mathbf{q})^2 - \Omega_{\mu} - M_2(\omega, \mathbf{k} + \mathbf{q})}, \end{aligned} \quad (6)$$

where

$$M_2(\omega, \mathbf{k} + \mathbf{q}) \equiv \sum_{\mu_1, \mathbf{q}_1} \frac{2|F_{\mu_1}(\mathbf{q}_1)|^2}{\hbar\omega - E - \frac{\hbar^2}{2m_0}(\mathbf{k} + \mathbf{q} + \mathbf{q}_1)^2 - \Omega_\mu - \Omega_{\mu_1}}; \quad (7)$$

$$\Omega_\mu = \begin{cases} \Omega_l, & \text{при } \mu = L_l; \\ \Omega_\pm, & \text{при } \mu = I_{s\pm}; \end{cases}$$

($l = 0, 1$; and Ω_\pm are the averaged energies of symmetric interface phonons).

Passing in (7) from the summation over the vector \mathbf{q}_1 to the integration over the variables (q_1, φ) of the polar coordinate system at $\mathbf{k} = 0$, one obtains

$$M_2(\omega, q) = \frac{S}{2\pi^2} \sum_{\mu_1} \int_0^{q_{\max}} q_1 |F_{\mu_1}(q_1)|^2 dq_1 \times \int_0^{2\pi} \frac{d\varphi}{\hbar\omega - E - \frac{\hbar^2}{2m_0}(\mathbf{q} + \mathbf{q}_1)^2 - \Omega_\mu - \Omega_{\mu_1}}. \quad (8)$$

The integral over the variable φ can be taken accurately, which results in the function

$$J_{\mu, \mu_1}(\omega, q, q_1) = -2\pi \left\{ \left[\hbar\omega - E - \frac{\hbar^2}{2m_0}(q^2 + q_1^2) - \Omega_\mu - \Omega_{\mu_1} \right]^2 - \left[\frac{\hbar^2 q q_1}{m_0} \right]^2 \right\}^{-1/2}, \quad (9)$$

Using the explicit form of the EPI functions, one can put down

$$M_2(\omega, q) = \frac{2e^2}{a} C \sum_{\mu} \left\{ \frac{\pi \Omega_{L_0}}{\varepsilon^{(0)}} \times \sum_{\lambda=1}^N (\lambda X_\lambda)^2 \int_0^{\pi/a_0} \frac{J_{L_0, \mu}(\omega, q, q_1) q_1 dq_1}{q_1^2 + (\lambda\pi/a)^2} + a \sum_{p=\pm} \Omega_p \int_0^{\pi/a_0} \frac{J_{sp, \mu}(\omega, q, q_1) f_s^2(q_1) dq_1}{\varepsilon_s^{(0)}(q_1) \zeta_{sp}^{(0)}(q_1) + \varepsilon_s^{(1)}(q_1) \zeta_{sp}^{(1)}(q_1)} + \right.$$

$$\left. + \frac{2a_1^3 \Omega_{L_1}}{\pi^2 a \varepsilon^{(1)}} \cos^4 \frac{k_0 a}{2} \int_0^{\pi/a_1} J_{L_1, \mu}(\omega, q, q_1) I(q_1) q_1 dq_1 \right\}, \quad (10)$$

where

$$C = \frac{4}{\left[1 + \frac{\sin(k_0 a)}{k_0 a} + 2 \frac{\sin^2(k_0 a/2)}{k_1 a} \right]^2}; \quad \frac{1}{\varepsilon^{(l)}} = \frac{1}{\varepsilon_\infty^{(l)}} - \frac{1}{\varepsilon_0^{(l)}};$$

$$\varepsilon_s^{(l)}(q) = \varepsilon_\infty^{(l)} [1 - (-1)^l \exp(-qa)];$$

$$\zeta_{sp}^{(l)}(q) = \frac{\varepsilon^{(l)} \Omega_{sp}^2(q)}{\varepsilon_0^{(l)} \Omega_{T_l}^2} \left[\frac{\Omega_{L_l}^2 - \Omega_{T_l}^2}{\Omega_{T_l}^2 - \Omega_{sp}^2(q)} \right]^2;$$

$$I(q) = \int_0^{\pi/a_1} \frac{a_1 q_\perp^2 dq_\perp}{(q^2 + q_\perp^2)[(2k_1 a_1)^2 + (q_\perp a_1)^2]^2}; \quad (11)$$

$$k_0 = \sqrt{2m_0 E}/\hbar, \quad k_1 = \sqrt{2m_1(V - E)}/\hbar,$$

while X_λ and $f_s(q)$ are the functions given in [11] that depend on the NF thickness a and the transverse component of the electron quasimomentum k_l in medium l ($l = 0, 1$) present in the corresponding coupling function. In particular, within the used model,

$$X_\lambda = \frac{1 - (-1)^\lambda}{2} \left[\frac{1}{(\lambda\pi)^2} + \frac{\cos(k_0 a)}{(\lambda\pi)^2 - (2k_0 a)^2} \right],$$

$$f_s(q) = \frac{\sqrt{1 + \exp(-qa)}}{a} \left\{ \frac{2 \cos^2(k_0 a/2)}{2k_1 + q} + \text{th} \left(\frac{qa}{2} \right) \left[\frac{q \cos(k_0 a)}{4k_0^2 + q^2} + \frac{1}{q} \right] + \frac{2k_0 \sin(k_0 a)}{4k_0^2 + q^2} \right\}.$$

One should also take into account that the main contribution into the MO is made by states with small values of the quasimomentum [11], whereas function (9) has partial derivatives of arbitrary order. Expanding it into a series and keeping the terms of the second and lower order, we integrate (10) over q_1 and obtain

$$M_2(\omega, q) = M_2^{(0)}(\omega) + M_2^{(2)}(\omega) q^2, \quad (12)$$

where

$$M_2^{(i)}(\omega) = -\frac{4e^2 m_0 a}{\hbar^2} C \sum_{\mu} \left\{ \frac{\Omega_0}{\varepsilon^{(0)}} \sum_{\lambda=1}^N (\lambda X_\lambda)^2 Y_{\lambda\mu}^{(i)}(\omega) + \right.$$

$$+ \frac{2a}{\pi^2} \sum_{p=\pm} \Omega_p Z_{p\mu}^i(\omega) + \frac{2\Omega_1}{\pi\varepsilon^{(1)}} \cos^4\left(\frac{k_0 a}{2}\right) I(0) W_\mu^{(i)}(\omega) \Big\}; \quad (13)$$

$$Y_{\lambda\mu}^{(0)}(\omega) = \frac{N^2 \eta_{L_0\mu}(\omega)}{\lambda^2 \eta_{L_0\mu}(\omega) + 1} \ln \frac{1 - N^2 \eta_{L_0\mu}(\omega)}{1 + (N/\lambda)^2};$$

$$Y_{\lambda\mu}^{(2)}(\omega) = \frac{a^2}{\pi^2} \left\{ \frac{2\eta_{L_0\mu}(\omega)}{[\lambda^2 \eta_{L_0\mu}(\omega) + 1]^3} \ln \frac{1 - N^2 \eta_{L_0\mu}(\omega)}{1 + (N/\lambda)^2} + \right.$$

$$+ \frac{N^2 \eta_{L_0\mu}^2(\omega)}{[\lambda^2 \eta_{L_0\mu}(\omega) + 1]^2} \left[\frac{2N^2 \eta_{L_0\mu}(\omega)}{N^2 \eta_{L_0\mu}(\omega) - 1} - \right.$$

$$\left. - \ln \frac{1 - N^2 \eta_{L_0\mu}(\omega)}{1 + (N/\lambda)^2} \right] -$$

$$\left. - \frac{N^4 \eta_{L_0\mu}^3(\omega)}{[\lambda^2 \eta_{L_0\mu}(\omega) + 1][N^2 \eta_{L_0\mu}(\omega) - 1]^2} \right\};$$

$$Z_{p\mu}^{(0)}(\omega) = \int_0^{\pi/a_0} \frac{\eta_{p\mu}(\omega)}{(qa/\pi)^2 \eta_{p\mu}(\omega) - 1} \times$$

$$\times \frac{f_s^2(q) dq}{\epsilon_s^{(0)}(q) \zeta_{sp}^{(0)}(q) + \epsilon_s^{(1)}(q) \zeta_{sp}^{(1)}(q)};$$

$$Z_{p\mu}^{(2)}(\omega) = \frac{a_0^2}{\pi^2} \int_0^{\pi/a_0} \left[\frac{1}{[(qa/\pi)^2 \eta_{p\mu}(\omega) - 1]^2} + \right.$$

$$\left. + \frac{2}{[(qa/\pi)^2 \eta_{p\mu}(\omega) - 1]^3} \right] \eta_{p\mu}^2(\omega) \times$$

$$\times \frac{f_s^2(q) dq}{\epsilon_s^{(0)}(q) \zeta_{sp}^{(0)}(q) + \epsilon_s^{(1)}(q) \zeta_{sp}^{(1)}(q)};$$

$$W_\mu^{(0)}(\omega) = \left(\frac{a_1}{a}\right)^3 \ln \left[1 - \left(\frac{a}{a_1}\right)^2 \eta_{L_1\mu}(\omega) \right];$$

$$W_\mu^{(2)}(\omega) = \frac{aa_1}{\pi^2} \left[\frac{a_1^2 \eta_{L_1\mu}(\omega)}{a^2 \eta_{L_1\mu}(\omega) - a_1^2} \right]^2;$$

$$\eta_{\mu\mu_1}(\omega) = \frac{\pi^2 \hbar^2}{2m_0 a^2 (\hbar\omega - E - \Omega_\mu - \Omega_{\mu_1})},$$

and it is set

$$I(q_1) \approx I(0) = \frac{1}{8\pi(k_1 a)^2} \left[\frac{1}{(2k_1 a_1/\pi)^2 + 1} + \frac{\pi}{2k_1 a_1} \operatorname{arctg} \frac{\pi}{2k_1 a_1} \right].$$

With the use of these notations, the total MO takes the form

$$M(\omega) = -\frac{\pi e^2}{a} C \left\{ \frac{\pi}{\varepsilon^{(0)}} \sum_{\lambda=1}^N (\lambda X_\lambda)^2 \Phi_\lambda(\omega) + \frac{aa_0^2}{2\pi^3} \times \right.$$

$$\times \sum_{p=\pm} \frac{\Omega_p \eta_{sp}(\omega)}{\hbar^2/(2m_0) + M_2^{(2)}(\omega)} \int_0^{\pi/a_0} \frac{1}{(qa_0/\pi)^2 \eta_{sp}(\omega) - 1} \times$$

$$\times \frac{f_s^2(q) dq}{\epsilon_s^{(0)}(q) \zeta_{sp}^{(0)}(q) + \epsilon_s^{(1)}(q) \zeta_{sp}^{(1)}(q)} +$$

$$\left. + \frac{2a_1^3 \Omega_1}{\pi^2 a \varepsilon^{(1)}} \cos^4\left(\frac{k_0 a}{2}\right) I(0) \frac{\ln[1 - \eta_{L_1}(\omega)]}{\hbar^2/(2m_0) + M_2^{(2)}(\omega)} \right\}, \quad (14)$$

where

$$\Phi_\lambda(\omega) = \frac{\Omega_0 \eta_{L_0}(\omega) a_0^2}{\pi^2 [\hbar^2/(2m_0) + M_2^{(2)}(\omega)]} \frac{\ln \frac{1 - \eta_{L_0}(\omega)}{1 + (N/\lambda)^2}}{(\lambda/N)^2 \eta_{L_0}(\omega) + 1};$$

$$\eta_\mu(\omega) = \frac{\pi^2}{a_\mu^2} \frac{\hbar^2/(2m_0) + M_2^{(2)}(\omega)}{\hbar\omega - E - \Omega_\mu - M_2^{(0)}(\omega)};$$

$$a_\mu = \begin{cases} a_0, & \text{при } \mu = L_0, I_s \pm; \\ a_1, & \text{при } \mu = L_1. \end{cases}$$

The position of the electron main-band bottom renormalized by EPI in a nanofilm is determined by the state density

$$g(\omega) = \frac{\operatorname{Im} M(\omega)}{[\hbar\omega - E - \operatorname{Re} M(\omega)]^2 + [\operatorname{Im} M(\omega)]^2}. \quad (15)$$

In the region $\hbar\omega \leq E$, it can be found from the equation

$$\hbar\omega - E = M(\omega). \quad (16)$$

Above the band bottom, the components of the two-phonon MO $M_2(\omega, q)$ can take on complex values, while the ranges of real values for each of them are different. The total MO $M(\omega)$ becomes, respectively, complex as well. Separating its real and imaginary parts, one can find the density of bound electron-phonon states $g(\omega)$.

3. Results and Discussion

Our calculations were performed for a β -HgS nanofilm surrounded by bulky medium β -CdS with the use of the parameters of the system given in [11].

Figure 1, *a* shows the spectral dependences of the real and imaginary parts of the MO calculated in the one-phonon (dashed lines) and two-phonon (solid lines) approximations for a nanofilm 2.34 nm in thickness ($N = 4$). One can see that the shift of the main-band bottom ($\Delta^{(2)} = -0.371\Omega_0$) determined in the two-phonon approximation exceeds the corresponding value ($\Delta^{(1)} = -0.321\Omega_0$) obtained with the use of the one-phonon one. The imaginary parts of the MO differ in positions and heights of the peaks as well.

The energy dependences of the bound state density calculated in the both approximations are presented in Fig. 1, *b, c*. The delta-like peak and local maxima of the curve $g(\omega)$ determine the positions of the band bottom and first-order phonon replicas, respectively.

In the framework of the one-phonon approximation, replicas related to each of the phonon branches are determined by the energy of a corresponding phonon Ω_μ , whereas the band bottom shifts to the long-wavelength region by the distance $\Delta^{(1)}$. As a result, each phonon replica appears at the distance $|\Delta^{(1)}| + \Omega_\mu$ from the band bottom, which exceeds the energy of the corresponding phonon.

Refining the position of the band bottom, the two-phonon approximation determines the energies of bound electron-phonon states renormalized by the interaction with phonons. According to the performed calculations, the shift of each peak of the state density corresponding to a certain phonon replica exceeds the shift increment of the band bottom $\Delta^{(1)} - \Delta^{(2)}$. That is why the distance of each phonon replica from the band bottom decreases, by approaching the value of Ω_μ . This fact is illustrated by Fig. 1, *b*, where the dashed line shows the peak of the phonon replica I_{s+} determined in the two-phonon approximation with regard for the interaction exclusively with the high-energy branch of symmetric interface phonons. The shifts of the peaks corresponding to other branches are similar though much smaller in magnitude.

The use of the two-phonon MO with regard for the interaction of an electron with all phonon branches in a nanofilm results in the fact that the state density (thick solid line in Fig. 1, *b*) differs from the simple superposition of its partial components, one of which (I_{s+}) is shown by the dashed line. One can see that the mutual influence of different branches of the phonon spectrum in a nanofilm

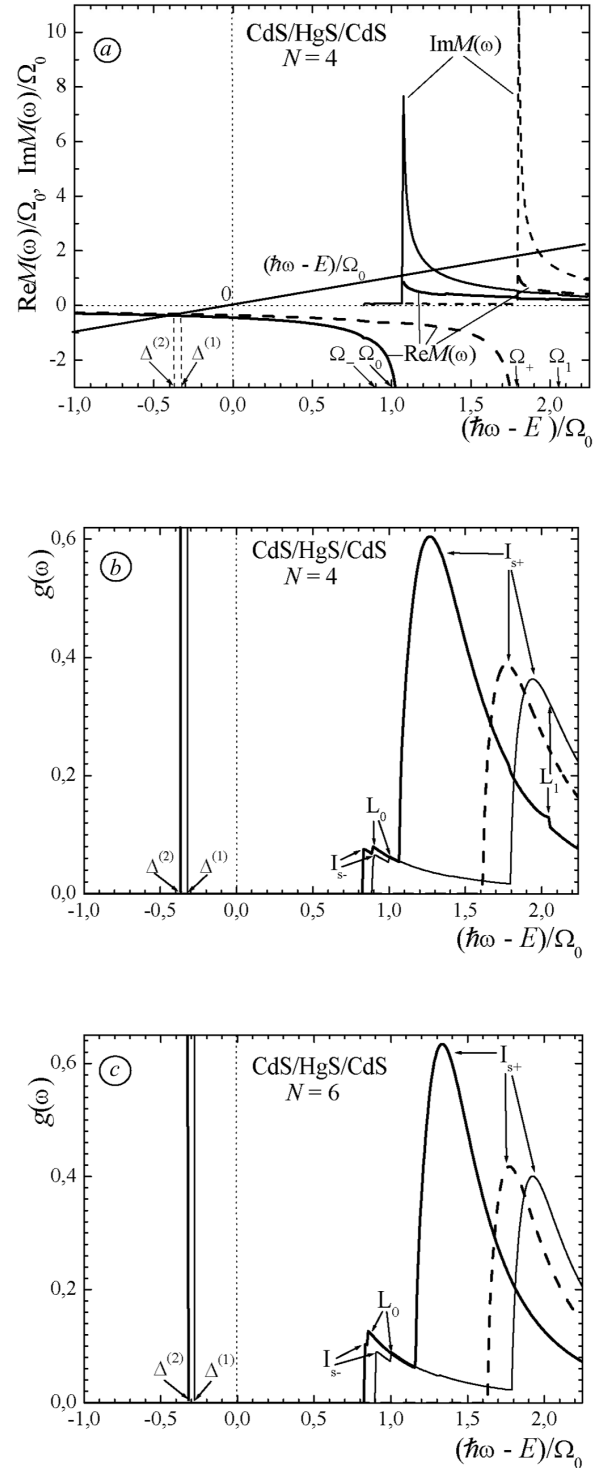


Fig. 1. Spectral dependences of the real and imaginary parts of the mass operator in the one- (dashed lines) and two-phonon (solid lines) approximations (*a*) and bound state densities in the one- (thin lines) and two-phonon (thick lines) approximations (*b, c*)

manifests itself in a nonlinear shift of the maxima and the widening of each peak of the function $g(\omega)$. The latter fact testifies to a decrease of the lifetime of the corresponding bound state due to the interaction with all phonon branches in a nanofilm.

Figure 1, *c* presents the results of similar calculations performed for a nanofilm of larger width (3.51 nm, $N = 6$). One can see that the positions of the electron main-band bottom and phonon replicas depend on the thickness of the nanofilm: its increase results in the growth of the state density related to confined phonons and a decrease of that related to half-space ones. The relative height of the corresponding maxima and their positions (and, therefore, the form of Raman spectra in a nanofilm) will considerably depend on its thickness. This fact gives one a possibility to control the geometry of nanoheterosystems by means of Raman spectroscopy methods.

Table summarizes the results of calculation of the shifts of the main-band bottom of an electron in QW performed in the one- and two-phonon approximations with regard for EPI with exclusively confined phonons for a number of nanofilms with different electron-phonon coupling constants

$$\alpha_F = \frac{e^2}{\hbar} \left(\frac{1}{\varepsilon_\infty} - \frac{1}{\varepsilon_0} \right) \sqrt{\frac{m}{2\Omega}}.$$

One can see that, for a nanofilm with the weak electron-phonon coupling, the difference between the results obtained in the one- and two-phonon approximations is small (not exceeding 15%) and decreases with decrease in α_F . This fact gives grounds to state that the use of the one-phonon approximation for the calculation of the energy of an electron in QW renormalized due to its interaction with phonons in nanosystems with the weak electron-phonon coupling is quite reasonable.

4. Conclusions

1. We have proposed a theory that allows one to consistently describe, for the first time, the role of two-phonon processes in the formation of the energy spectrum of an electron with regard for its interaction with all types of optical polarization phonons in a nanofilm.

Nanofilm	α_F	$\Delta^{(1)}/\Omega$	$\Delta^{(2)}/\Omega$	Difference, %
InP/InAs/InP	0.048	-0.0270	-0.0274	1.5
AlAs/GaAs/AlAs	0.079	-0.0482	-0.0496	2.6
ZnS/CdS/ZnS	0.139	-0.0882	-0.0923	4.6
β -CdS/ β -HgS/ β -CdS	0.497	-0.2796	-0.3199	14.4

2. It is shown that, in a nanofilm with the weak electron-phonon coupling, the difference between the results of calculation of the electron energy in the one- and two-phonon approximations is small. But the positions of the first phonon replicas of Raman spectra in a nanofilm can be obtained only using an approximation taking at least two-phonon processes into account.

3. In order to obtain the positions of the next phonon replicas at $T = 0$ K, the EPI theory developed in the two-phonon approximation can be generalized to a wider energy interval by means of considering the multiphonon processes. The use of the Pines diagram technique at small electron concentrations will also give a possibility to adopt this theory to the case of arbitrary temperatures, which is supposed to be done in our following works.

1. P. Harrison, *Quantum Wells, Wires, and Dots: Theoretical and Computational Physics* (Wiley, Chichester, 1999).
2. V.V. Mitin, V.A. Kochelap, and M.A. Strosio, *Quantum Heterostructures. Microelectronics and Optoelectronics* (Cambridge Univ. Press, Cambridge, 1999).
3. D.D. Nolte, *J. Appl. Phys.* **85**, 6259 (1999).
4. D. Dorfs, H. Henschel, J. Kolny, and A. Eychemuller, *J. Phys. Chem. B* **108**, 1578 (2004).
5. P. Mohan, J. Motohisa, and T. Fukui, *Appl. Phys. Lett.* **88**, 133105 (2006).
6. L. Wendler, *Phys. Stat. Sol. (b)* **129**, 513 (1985).
7. K. Huang and B.F. Zhu, *Phys. Rev. B* **38**, 13377 (1988).
8. N. Mori and T. Ando, *Phys. Rev. B* **40**, 6175 (1989).
9. V.I. Boichuk and V.A. Borusevych, *Zh. Fiz. Dosl.* **10**, 39 (2006).
10. V.I. Boichuk, V.A. Borusevych, and I.S. Shevchuk, *J. Optoelectron. Adv. Mater.* **10**, 1357 (2008).
11. M.V. Tkach and V.M. Kramar, *Ukr. J. Phys.* **53**, 810 (2008).
12. M.V. Tkach and V.M. Kramar, *Ukr. J. Phys.* **53**, 1110 (2008).
13. A.A. Abrikosov, L.P. Gor'kov, I.E. Dzyaloshinsky, *Methods of Quantum Field Theory in Statistical Physics* (Dover, New York, 1975).
14. M.V. Tkach, *Quasiparticles in Nanoheterosystems. Quantum Dots and Wires* (Chern. Nats. Univ., Chernivtsi, 2003).
15. M.V. Tkach, *Zh. Fiz. Dosl.*, **6**, 124 (2002).

Received 03.08.09.

Translated from Ukrainian by H.G. Kalyuzhna

ЕНЕРГЕТИЧНИЙ СПЕКТР ЕЛЕКТРОНА З ФОНОННИМИ
ПОВТОРЕННЯМИ У ПЛОСКІЙ НАПІВПРОВІДНИКОВІЙ
НАНОГЕТЕРОСТРУКТУРІ З КВАНТОВОЮ ЯМОЮ

В.М. Крамар, М.В. Ткач

Р е з ю м е

Досліджено перенормування енергетичного спектра електрона у плоскій напівпровідниковій наногетероструктурі з прямоку-

тною квантовою ямою скінченної глибини внаслідок взаємодії з оптичними поляризаційними фононами. У рамках методу функцій Гріна одержано аналітичний вигляд масового оператора, де враховано двофононні процеси електрон-фононної взаємодії при $T = 0$ К. Обчислено поправку до енергії дна основної зони електрона та положення перших фононних повторень, викликаних його взаємодією з обмеженими, напівпросторовими та інтерфейсними фононами.